JGR Atmospheres

RESEARCH ARTICLE
10.1029/2019JD031982

Key Points:
- Heavy rainfall with daily precipitation greater than 20 mm contributes most to the occurrence of dry-wet abrupt alternation events
- Abrupt alternation between wet and dry spells is projected to occur more frequently over a larger spatial extent by the end of the 21st century
- Abrupt alternation (dry-wet-dry) is expected to occur due to the increasing number of heavy rainfall and drought events in a changing climate

Supporting Information:
- Supporting Information S1

Correspondence to:
S. Wang,
shuo.s.wang@polyu.edu.hk

Citation:
Chen, H., Wang, S., & Wang, Y. (2020). Exploring abrupt alternations between wet and dry conditions on the basis of historical observations and convection-permitting climate model simulations. *Journal of Geophysical Research: Atmospheres*, *125*, e2019JD031982. https://doi.org/10.1029/2019JD031982

Received 5 NOV 2019
Accepted 24 APR 2020
Accepted article online 26 APR 2020

Exploring Abrupt Alternations Between Wet and Dry Conditions on the Basis of Historical Observations and Convection-Permitting Climate Model Simulations

H. Chen[1], S. Wang[1,2], and Y. Wang[3]

[1]Department of Land Surveying and Geo-Informatics, The Hong Kong Polytechnic University, Hong Kong, [2]The Hong Kong Polytechnic University Shenzhen Research Institute, Shenzhen, China, [3]Department of Geosciences, Texas Tech University, Lubbock, TX, USA

Abstract Exploring the dynamic evolution of the abrupt alternation between wet and dry spells in adjacent months plays a crucial role in water resources planning and agricultural development in a changing climate. The dry-wet abrupt alternation (DWAA) has been studied based on hydrometeorological observations over the past several years. However, little effort has been made to explore DWAA from a climate projection standpoint. Furthermore, few studies have investigated potential interrelationships between DWAA and heavy rainfall. In this study, the interrelationships between DWAA events and heavy rainfall with various intensities as well as potential evapotranspiration are revealed explicitly through the convection-permitting climate simulations for 10 climate divisions over Texas in the United States. Our findings disclose that the increasing heavy rainfall and potential evapotranspiration lead to more frequent occurrence of DWAA events over a larger spatial extent. Heavy rainfall with daily precipitation greater than 20 mm contributes most to the occurrence of DWAA. In addition, a severe phenomenon of dry-wet-dry alternation is projected to appear due to the increasing number of heavy rainfall and drought events as well as the deteriorated soil water holding capacity under global warming.

Plain Language Summary The dry-wet abrupt alternation (DWAA) has dramatic negative impacts on water security and agricultural production. DWAA is a devastating natural disaster which is characterized by an abrupt alternation between wet and dry spells in adjacent months. Exploring the underlying mechanism and complex evolution of DWAA is thus crucial to helping policymakers and stakeholders develop sound adaptation and mitigation plans for reducing potential risks of natural extreme events. We find that the DWAA event is projected to occur simultaneously in multiple climate divisions, especially for the most populous region of South Texas. Heavy rainfall with daily precipitation greater than 20 mm contributes most to the occurrence of DWAA. Due to the increasing number of drought and heavy rainfall events, a severe super extreme event of the dry-wet-dry alternation is projected to appear by the end of this century, whereas there is no historical record on the occurrence of such an extreme event over Texas in the period of 1981–1995.

1. Introduction

Dry-wet abrupt alternation (DWAA) is an extreme event in which the alternation of dry and wet spells occurs abruptly (Shan et al., 2018; Wu et al., 2006). The abrupt alternation of dry and wet spells has substantial impacts on agriculture production and economic development (De Silva & Kawasaki, 2018), which can bring destructive consequences, such as soil erosion (Schmidt et al., 2006), land degradation (Cordova, 2000; Handwerger et al., 2019), and significant economic losses (Du et al., 2013).

DWAA is one of the most devastating natural disasters, which can be caused by complex interrelationships of drought and heavy rainfall. Drought is a large-scale and long-term natural hazard; by contrast, heavy rainfall occurs at a relatively small spatial scale over a short period of time. The occurrence of individual drought and heavy rainfall events has been extensively investigated over the past few decades (Malik et al., 2016; Nalbantis & Tsakiris, 2009; Zhang et al., 2019). Previous studies have indicated that the intense rainfall episodes may terminate droughts (Mo, 2011), and a long-lasting drought can be interrupted by extreme wet spells (Clark et al., 2009), which can result in the occurrence of DWAA. However, little effort has been

made to explore potential interrelationships of the large-scale drought and the small-scale heavy rainfall with different intensities even though the disastrous DWAA has received increasing attention from the hydroclimate community in recent years.

The DWAA events have been explored based on hydrometeorological observations over the past several years (Dong et al., 2011; Ji et al., 2018; Katsanos et al., 2018; Malik et al., 2016). For instance, Wu et al. (2006) investigated the droughts-floods coexistence phenomenon during the normal summer monsoons. Zhang et al. (2012) conducted a thorough investigation on the wetness and dryness variations during 1961–2008 in Xinjiang which is a region in northwest China with an arid climate. Du et al. (2013) investigated the spatiotemporal variation of dry/wet condition and the changing trend with the standardized precipitation index. Singh et al. (2014) examined the observed changes in extreme wet and dry spells during the South Asian summer monsoon season. Christian et al. (2015) quantified the frequency distribution of dipole events in which a drought year was followed by a pluvial year within the Oklahoma climate divisions during 1896–2013. Previous studies have mainly focused on investigating the transition of dry and wet spells from an observational perspective, but little effort has been made to examine the DWAA events from a climate projection standpoint.

Climate change intensifies the hydrological cycle, leading to an increasing temporal and spatial heterogeneity of precipitation and thus an increasing frequency of the concurrence of drought and heavy rainfall events. Previous studies have indicated that an increasing trend of heavy rainfall is expected at the expense of light to moderate rainfall in a warming environment (Mishra & Liu, 2014; Wang et al., 2017; Zhu et al., 2019). Such a changing precipitation pattern would result in an increasing number of dry days and an intensified heavy rainfall system (Mishra & Liu, 2014; Wang & Wang, 2019), thereby causing more frequent occurrence of the DWAA events as expected. In addition, the convection-permitting climate modeling system can be used as a powerful tool to well simulate the spatial and temporal variability of rainfall, especially for heavy rainfall (Prein et al., 2016). It is thus desired to conduct a robust assessment and projection of the DWAA evolution at a convection-permitting scale in order to advance the understanding of emerging extreme events and to develop sound mitigation and adaptation strategies.

The objective of this study is to explore the complex evolution of DWAA events for 10 climate divisions over Texas through the convection-permitting climate simulations and the use of the standardized precipitation evapotranspiration index (SPEI). The interrelationships of various types of DWAA and heavy rainfall with different intensities will also be revealed thoroughly. In addition, the convection-permitting climate model will be used to project the future changes of the DWAA characteristics over Texas in a changing climate.

This paper is organized as follows. Section 2 will introduce the study area, data, model, and extreme indices as well as the definition of DWAA used in this study. In section 3, the historical DWAA events will be reproduced, the interrelationships between various DWAA events and heavy rainfall with different intensity will be revealed, and the projected future changes of the DWAA characteristics will be depicted for 10 climate regions of Texas. In section 4, the occurrence of DWAA will be discussed and the DWAA changes in the metropolis area of Texas will be revealed. In section 5, the primary novelty of this work and the key findings will be highlighted.

2. Data Set, Model, and Method

2.1. Study Region and Data Set

Texas has been experiencing an increasing number of droughts and floods due to its location and climatic features (Wang et al., 2018; Yoon et al., 2018). Texas is located along 30° north latitude, which is a climate transition zone called the Great American Desert. Texas receives most of the moisture from the warm Gulf of Mexico, and precipitation varies seasonally. Figure 1 shows the annual mean precipitation decreasing from east to west in Texas of the United States. In the late spring (April, May, and June), Texas normally receives the maximum rainfall caused by thunderstorm activities provoked by cold and warm fronts. Particularly in the western half of Texas, one or two rainstorms often account for nearly all of monthly rainfall. The second wettest months are September and October due to tropical cyclones developing in the Gulf of Mexico, the Caribbean Sea, and the Atlantic Ocean. These intense storms occasionally provide the moisture needed to quench serious droughts.

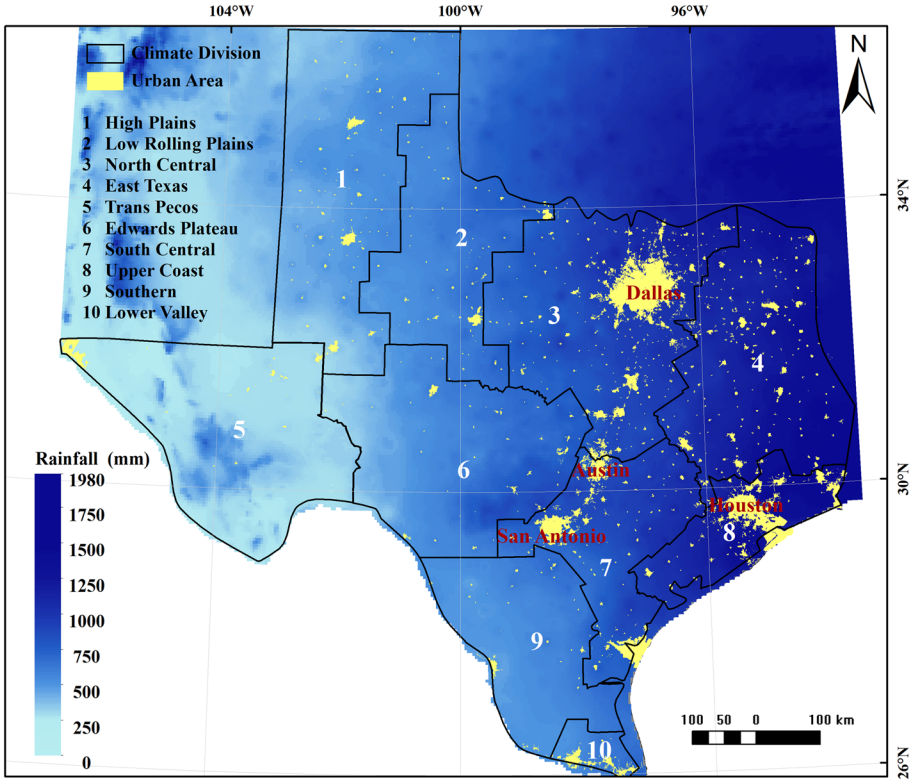

Figure 1. The WRF model domain and the spatial pattern of annual rainfall for 10 climate divisions of Texas including 1. High Plains; 2. Low Rolling Plains; 3. North Central; 4. East Texas; 5. Trans Pecos; 6. Edwards Plateau; 7. South Central; 8. Upper Coast; 9. Southern;10. Lower Valley. The urban areas are highlighted in yellow.

In addition, droughts vary in intensity and duration depending on how atmosphere and ocean interact, such as El Niño and La Niña that have a considerable impact on droughts in Texas. Previous studies reveal that a strong El Niño contributes to wetter-than-average winters and springs in Texas as it can shift the jet stream farther south into Texas and suppress tropical cyclone activities (Wang et al., 2015). By contrast, La Niña leads to drier-than-average conditions in Texas by shifting the jet stream north and enhances tropical cyclone activities. Moreover, Texas varies from the forests of the east and the Coastal Plain in the south to the elevated plateaus and basins in the north and west, which brings a wide variety of weather throughout the year. Due to the expansive and topographically diverse nature, Texas offers continental, marine, and mountain-type climates, and the region of Texas can be divided into 10 climate divisions (Figure 1).

In this study, the water deficit or surplus is estimated based on the difference between precipitation and potential evapotranspiration (PET). The climate diversity of Texas is beneficial to assess different wet/dry conditions in 10 climate divisions. Furthermore, the thunderstorm occurs frequently over Texas in the late spring, which often brings heavy rainfall. In the subsequent summer, Texas experiences a hot and dry period and then is followed by a rainfall peak in September and October. Such climatic features are prone to suffering from droughts and floods, which can increase the likelihood of occurrence of dry-wet (D-W) alternation events.

The Parameter-elevation Regressions on Independent Slopes Model (PRISM, http://www.prism.oregonstate.edu) data set has daily and monthly records of meteorological variables available at the 4-km resolution across the United States (Daly et al., 2008). The PRISM data set was used in this study to validate the Weather Research and Forecasting (WRF) climate model as well as to examine the temporal and spatial variability of various DWAA events and heavy rainfall with different intensities.

2.2. Convection-Permitting Climate Modeling

The WRF Model Version 3.7.1 was used to perform the convection-permitting climate simulations with a spatial resolution of 4 km (Skamarock et al., 2008). The study domain has 380 × 350 grid points which

covers a region of 1,520 km × 1,400 km with 51 stretched vertical levels topped at 50 hPa using a single domain. A 4-km horizontal grid spacing was configured in this study, which was fine enough to explicitly resolve the convection without the use of convection parameterization (Liu et al., 2011). The National Center for Environment Prediction Climate Forecast System Reanalysis (CFSR), available at a spatial resolution of 38 km and 6-hourly temporal resolution, was used to generate the initial and lateral boundary conditions. Two 15-year climate simulations were conducted for Texas. The historical climate simulation spans the period from 1981 to 1995, and the future projection spans the period from 2085 to 2099.

The physical parameterization schemes used in climate simulations include the Noah-MP land surface scheme (Niu et al., 2011; Yang et al., 2011), the Thompson cloud microphysics scheme (Thompson et al., 2008), the Yongsei University planetary boundary layer scheme (Hong & Pan, 1996), the rapid radiative transfer model shortwave and longwave radiation scheme (Iacono et al., 2008), and the revised Monin-Obukhov surface layer scheme (Jiménez et al., 2012) (please refer to Liu et al., 2017 for a detailed description on the aforementioned physical parameterization schemes).

The pseudo global warming (PGW) approach was applied to project future climate change information under the RCP8.5 emission scenario (Liu et al., 2017; Prein et al., 2016). The 15-year (2085–2099) WRF simulation was forced with the 6-hr CFSR and a climate perturbation which was estimated by subtracting the multigeneral circulation models (GCMs) ensemble mean of historical simulations (1976–2005) from the multi-GCMs ensemble mean of future projections (2071–2100) under the RCP 8.5 climate scenario (Rasmussen et al., 2017). The multimodel ensemble mean climate change signal enables us to exploit the large range of internal variability and climate sensitivity of GCMs (Wang & Zhu, 2020). It should be noted that the PGW approach is based on an assumption that the year-to-year and the short-term variation in the present climate is the same in the future. The lateral boundary conditions were perturbed by PGW to generate the ensemble mean climate change signal from 15 Coupled Model Intercomparison Project Phase 5 GCMs (see Table S1 of the supporting information). In this study, the time series of precipitation and PET were collected from the WRF simulations for the historical period of 1981–1995 and were projected for the future period of 2085–2099 through the convection-permitting climate simulation.

2.3. Extreme Indices

DWAA is mainly attributed to the spatial and temporal variations of precipitation, especially for the extreme precipitation that may terminate droughts abruptly. Since precipitation is the most essential factor affecting the onset and the termination of dry and wet spells, the potential interrelationships of DWAA and heavy rainfall events were examined using the extreme precipitation indices including R10–20, R20–25, and R25 (Frich et al., 2002). R10–20, R20–25, and R25 are defined as the grid-averaged cumulative number of days with daily precipitation ranging from 10 to 20, from 20 to 25, and larger than 25 mm, respectively. R10–20, R20–25, and R25 on a monthly basis are the commonly used indices for defining the frequency of extreme precipitation (Ahmed et al., 2013; Alexander et al., 2006; Azizzadeh & Javan, 2018; Guo et al., 2016). Thus, R10–20, R20–25, and R25 were used to investigate the contributions of heavy rainfall with different intensities to DWAA for 10 climate divisions of Texas.

The SPEI was used to assess climate change impacts on DWAA for 10 climate divisions of Texas. Similar to the standardized precipitation index approach (McKee et al., 1993), the SPEI was calculated based on the difference between monthly precipitation and PET (Vicente-Serrano et al., 2010). The PET was estimated by the FAO-56 Penman-Monteith equation (Allen et al., 2005). The difference between monthly precipitation and PET provides a metric of water surplus or deficit. According to Vicente-Serrano et al. (2010), the frequency of the difference at monthly time scales can be well modeled using the statistical distribution. In this study, the monthly difference over the 15-year period was combined and then the combined monthly difference was fitted to the best fitness theoretical distribution function. The probability of water surplus/deficit was then generated along with an estimate of the inverse normal to calculate the deviation of the difference between precipitation and PET for a normal distribution. Thus, the DWAA derived by SPEI represents the abrupt transition between meteorological dry and wet conditions in adjacent months.

2.4. DWAA

SPEI is used to characterize the meteorological water deficit/surplus conditions. The value of SPEI represents the standard deviation of standard normal distribution. The dry condition is represented by the SPEI

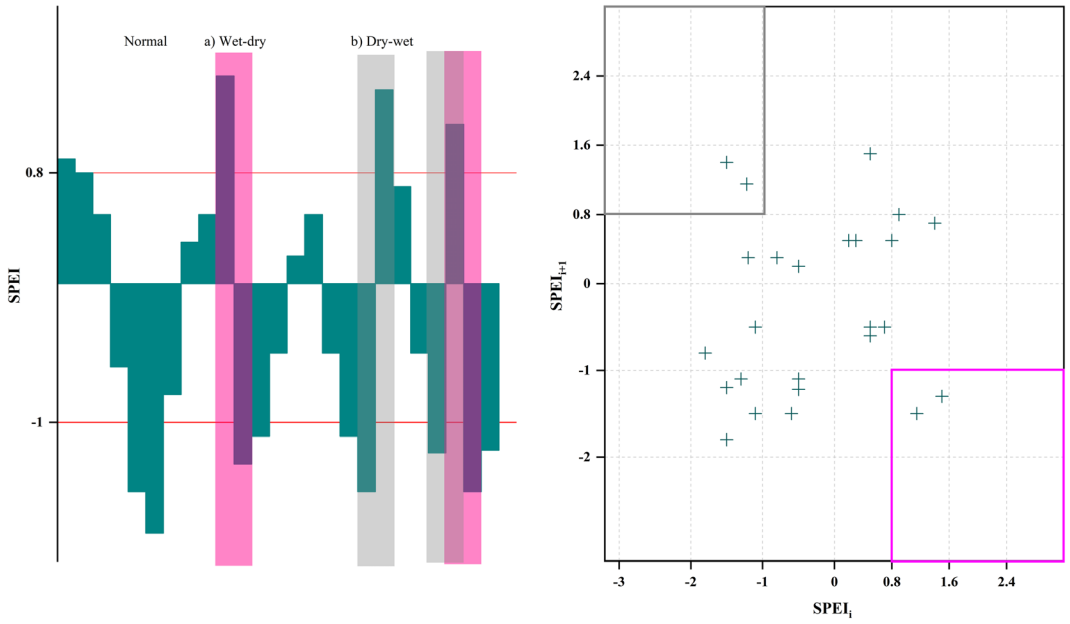

Figure 2. Definition of dry-wet abrupt alternation (DWAA) by SPEI; (a) wet-dry (W-D) alternation is indicated by the $SPEI_i$ value $\geq$0.8 in the *i*th month and the $SPEI_{i+1}$ value ≤ -1 in the $i+1$st month, which is represented by the points lying inside the pink rectangle; (b) dry-wet (D-W) alternation is indicated by the $SPEI_i$ value ≤ -1 and $SPEI_{i+1} \geq 0.8$, which is represented by the points lying inside the gray rectangle. The SPEI values shown in this Figure are used as an example for the identification of the W-D alternation and the D-W alternation events.

value less than −1, while the wet condition is indicated by the SPEI value greater than 0.8 (Mckee et al., 1993). It should be noted that the threshold was adjusted downward (from 1 to 0.8) to yield a greater sample size for providing more statistically robust results. DWAA represents dry (wet) conditions abruptly change to wet (dry) conditions in adjacent months. This study examines two different types of DWAA events defined as follows. First, when a wet spell ($SPEI_i \geq 0.8$) is followed by a dry spell ($SPEI_{i+1} \leq -1$) due to the precipitation deficit, this phenomenon is a wet-dry (W-D) alternation as indicated in Figure 2a and represented by the points lying inside the pink rectangle. Second, when a dry spell ($SPEI_i \leq -1$) abruptly turns into a wet spell ($SPEI_{i+1} \geq 0.8$) due to the occurrence of heavy rainfall, this phenomenon is a D-W alternation as depicted in Figure 2b and represented by the points lying inside the gray rectangle. Therefore, the potential interrelationships of two different types of DWAA including the W-D and the D-W alternation events and heavy rainfall with different intensities including R10–20, R20–25, and R25 as well as PET will be thoroughly explored to advance our understanding of the complex evolution of the emerging DWAA events and to develop adaptation strategies for minimizing risks and damages caused by extreme events.

3. Results Analysis

3.1. Reproduction of Historical DWAA

Figure 3 depicts the comparison of annual and seasonal patterns of precipitation differences between the WRF simulation and the PRISM observation as well as those between the CFSR reanalysis product and the PRISM observation. As for the WRF simulation, there is a slightly dry bias in South Texas and a wet bias in North Texas. In comparison, there is a much larger dry bias in North Texas and a larger wet bias in South Texas based on the CFSR reanalysis product. These results indicate that the convection-permitting WRF model has better performance in comparison with the CFSR product, especially for the simulation of summertime (June-July-August) precipitation. In fact, the convection-permitting climate model is recognized as a powerful means to well simulate the spatial and temporal variability of precipitation which is the most important climate variable affecting the DWAA events. Figure 4 presents the comparison of spatial distributions of the annual mean number of cumulative days of heavy rainfall with different intensities (R10–20,

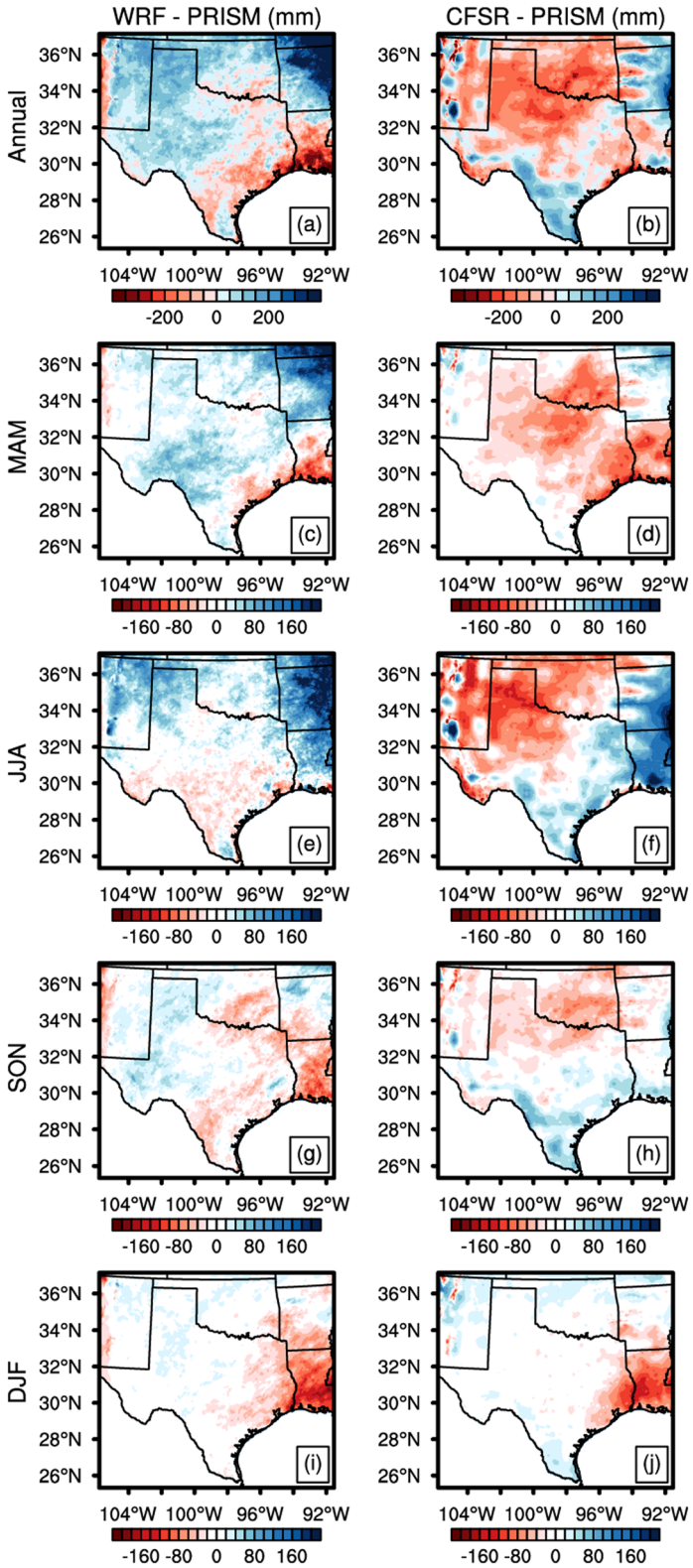

Figure 3. (a) Spatial pattern of 15-year annual mean precipitation difference between the WRF simulation and the PRISM observation. (b) Spatial pattern of 15-year annual mean precipitation difference between the CFSR reanalysis product and the PRISM observation. (c–j) Spatial distributions of seasonal mean precipitation differences between the WRF simulation and the PRISM observation as well as those between the CFSR reanalysis product and the PRISM observation.

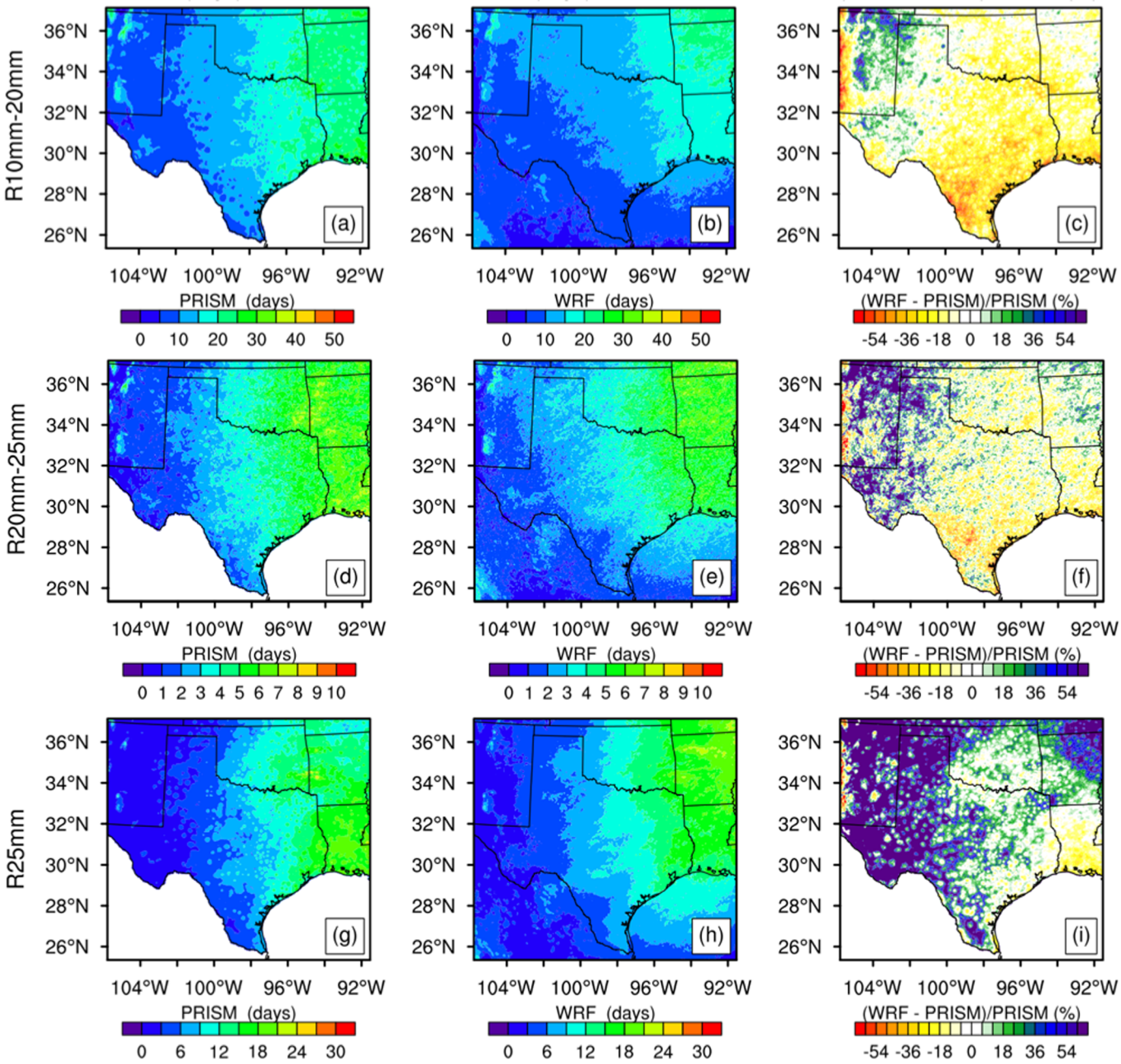

Figure 4. (a–j)Comparison of spatial distributions of annual mean number of days of heavy rainfall with different intensities (R10–20, R20–25, and R25) derived from the convection-permitting WRF climate simulation and the PRISM observation for the period of 1981–1995. The rows represent the rainfall intensities of R10–20, R20–25, and R25, respectively. The left to right columns represent the rainfall intensities derived from the PRISM observation, the WRF simulation, and the difference between WRF and PRISM, respectively.

R20–25, and R25) derived from the PRISM observation and the WRF simulation. As shown in Figures 4a and 4b, 4d and 4e, and 4g and 4h, there is a consistent spatial pattern of the annual mean number of rain days with three different intensities. And the number of heavy rain days is relatively small in West Texas and is increasing eastward.

According to the absolute difference between observed and simulated extreme precipitation under the R10–20 category (Figure 4c), the WRF model tends to underestimate the number of heavy rainfall events over Southeast Texas. As for the R20–25 category (Figure 4f), there is a slight difference between model

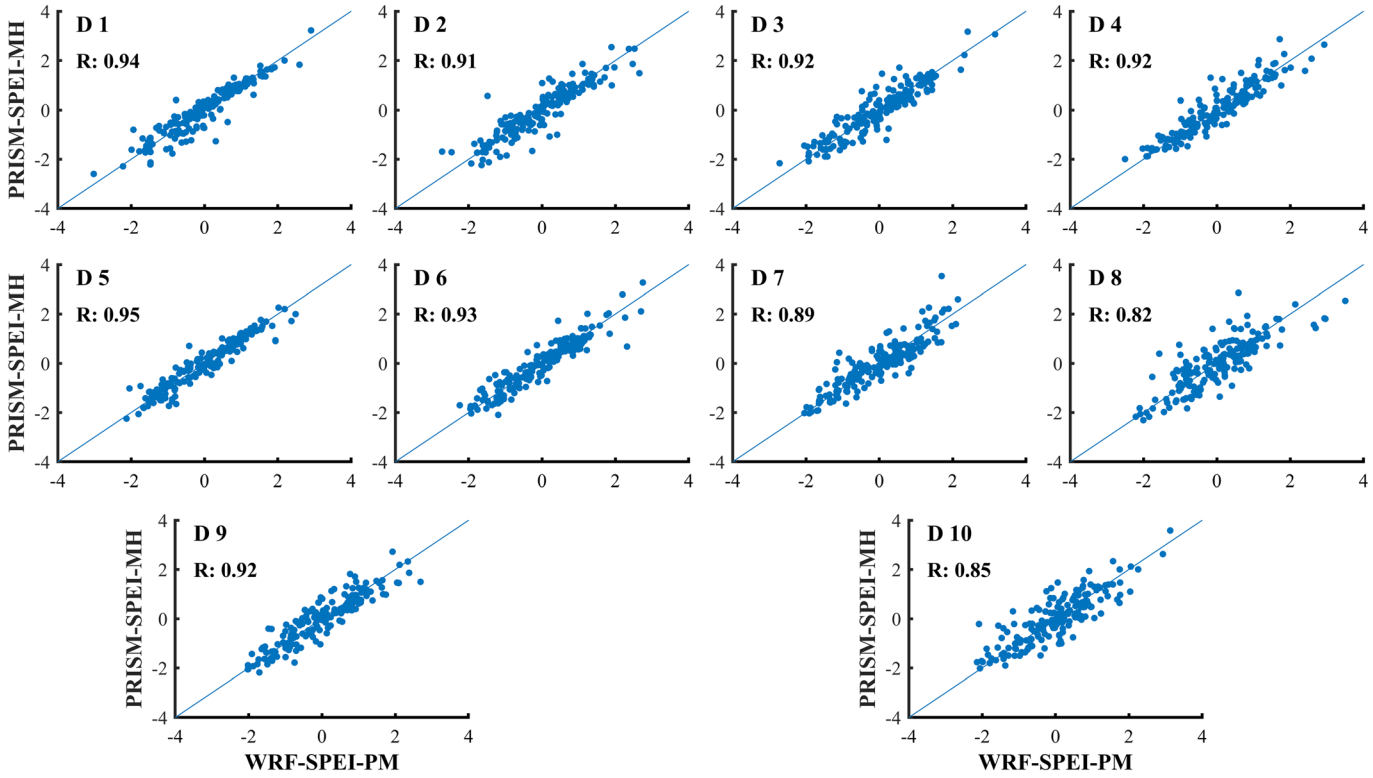

Figure 5. Comparison of SPEI values derived by the WRF simulation and the PRISM observation for the historical period of 1981–1995 over 10 climate divisions of Texas.

simulations and observations. As for the R25 category (Figure 4i), the WRF model tends to overestimate the number of heavy rain days over West Texas for where has slight heavy rain days. These results indicate that the convection-permitting WRF model is able to well capture the spatial pattern of heavy rainfall with different intensities over Texas. The accurate simulation of precipitation plays a crucial role in improving the reliability of assessing the DWAA events and their interrelationships with heavy rainfall.

Figure 5 depicts the comparison of monthly SPEI values derived from the WRF simulation based on the FAO-56 Penman-Monteith equation and the PRISM observation based on the Modified-Hargreaves equation for the historical period of 1981–1995 over 10 climate divisions of Texas. The description of the PET calculation is provided in the supporting information. The SPEI values derived from the WRF simulation show good agreement ($R > 0.80$) with those derived from the PRISM observation for all climate divisions. These results indicate that the WRF-derived SPEI is able to well assess the water deficit or surplus in Texas.

The DWAA events were examined by SPEI in this study. A sensitivity analysis of thresholds used to identify the DWAA events is shown in Figures S1 and S2, and a detailed discussion of relationships between various thresholds and the detected number of DWAA events is also provided in the supporting information. As shown in Figure 6, the points lying inside the gray rectangle represent a dry condition in the ith month and abruptly turn into a wet condition in the $i + 1$st month based on the derived SPEI values. A total of seven D-W alternation events is detected in the historical period of 1981–1995, including two in High Plains (Division 1), one in North Central (Division 3), one in Trans Pecos (Division 5), one in Edwards Plateau (Division 6), one in South Central (Division 7), and one in Lower Valley (Division 10). In addition, the points lying inside the pink rectangle represent the W-D alternation in which a wet condition occurs in the ith month and abruptly turns into a dry condition in the $i + 1$st month. A total of eight W-D alternation events is detected, including one in Low Rolling Plains (Division 2), one in Trans Pecos (Division 5), one in Edwards Plateau (Division 6), one in South Central (Division 7), two in Upper Coast (Division 8), and two in Lower Valley (Division 10).

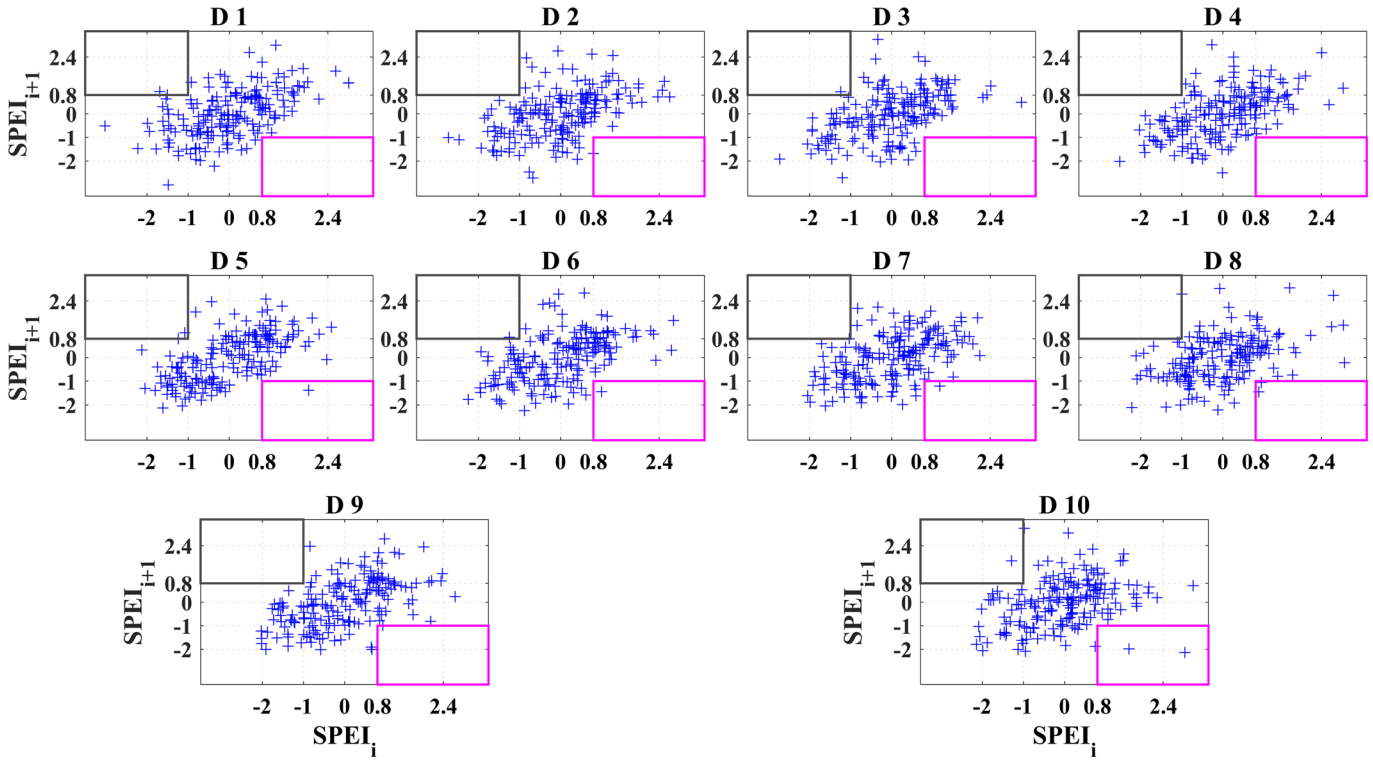

Figure 6. Historical DWAA events detected by SPEI for 10 climate divisions of Texas. The points lying inside the pink rectangle represent the occurrence of the W-D alternation event, while the points lying inside the gray rectangle represent the occurrence of the D-W alternation event.

To further improve the understanding of DWAA, the potential interrelationships of DWAA and heavy rainfall as well as PET were examined systematically. As shown in Figures 7 and 8, the Pearson correlation coefficient (*R* value) was used to estimate the correlation between DWAA and climatic variables for the 3 months before and after the occurrence of the DWAA events in the historical period from 1981 to 1995. Figure 7 presents the derived correlation coefficients with the significance level of 5% and the associated *p* values for assessing the interrelationships of W-D alternation events and climatic variables including monthly PET and the average number of monthly heavy rainfall days with different intensities (R10–20, R20–25, and R25). It can be seen that there is not a significant correlation between the monthly PET and the W-D alternation event at the significance level of 5%. However, there is a significant positive correlation between the W-D alternation event and heavy rainfall with different intensities. Furthermore, heavy rainfall with daily precipitation larger than 20 mm contributes most to the W-D alternation events. This indicates that the rapid reduction of heavy rainfall can terminate the meteorological wet condition and abruptly turn into the dry condition. As shown in Figure 8, there is a strong negative correlation between the D-W alternation event and the monthly PET, whereas there is no significant correlation between the D-W alternation event and heavy rainfall. This indicates that a strong correlation exists between PET and the D-W alternation event, and thus, the high PET has great potential risk of leading to the D-W alternation event. The interrelationships between the SPEI values and climatic variables are also depicted in Figures S3–S11 of the supporting information.

3.2. Projected Changes of DWAA

Future changes in the number of the DWAA events were assessed through the convection-permitting climate projection. Figure 9 presents the changes in the number of the DWAA events for the future period of 2085–2099 relative to the base period of 1981–1995. It can be seen that there is an increasing number of the D-W alternation events as highlighted by gray rectangles, especially for West (Division 5) and Southeast (Divisions 7–10) Texas. Moreover, there is a considerable increase in the number of the W-D alternation events as highlighted by pink rectangles for Central and South Texas (Divisions 4–10). North Texas

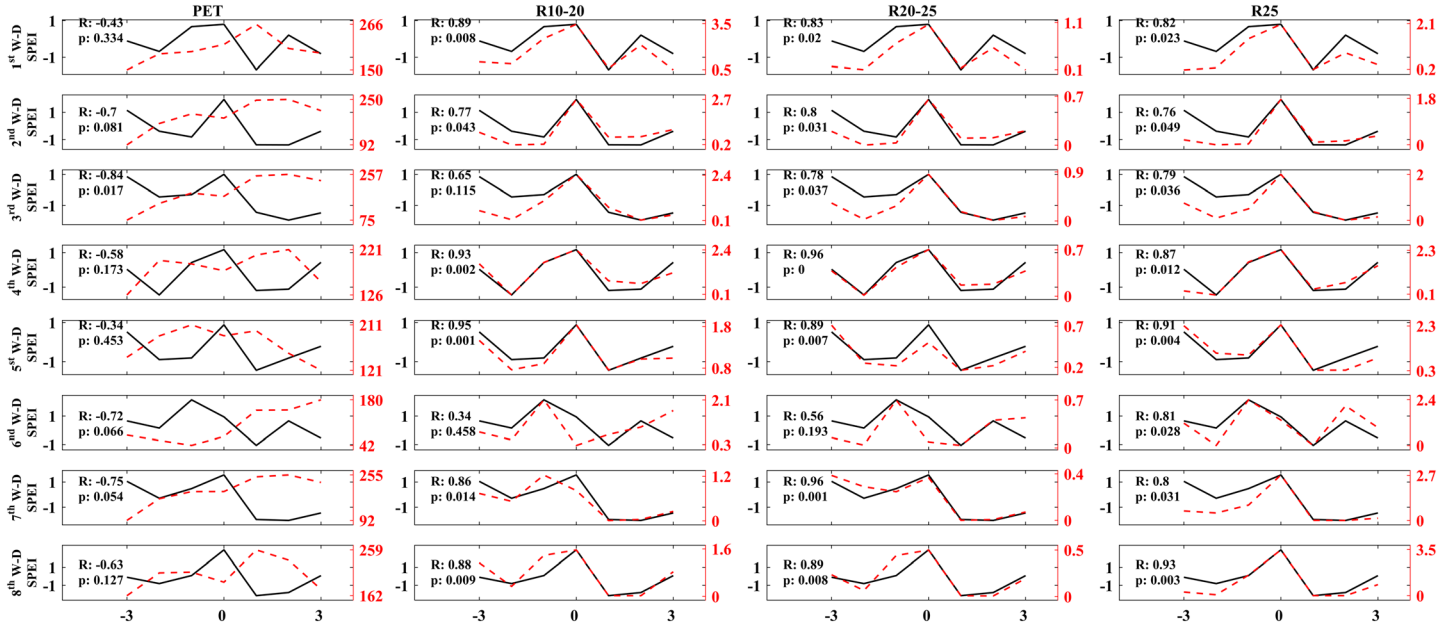

Figure 7. Interrelationships between wet-dry (W-D) alternation event and heavy rainfall with different intensities including R10–20, R20–25, and R25. Black lines represent the SPEI values. The red dashed lines represent the PET values in the first column, R10–20 values in the second column, which denotes the monthly number of days with daily precipitation ranging from 10 to 20 mm, R20–25 values in the third column, which denotes the monthly number of days with daily precipitation ranging from 20 to 25 mm, and R25 values in the fourth column, which denotes the monthly number of days with daily precipitation greater than 25 mm. *R* denotes the value of the Pearson correlation coefficient, and *p* denotes the *p* value derived by hypothesis testing with the significance level of 5%. The x ticks of −3 to 3 indicate 3 months before and 3 months after the occurrence of the W-D alternation event.

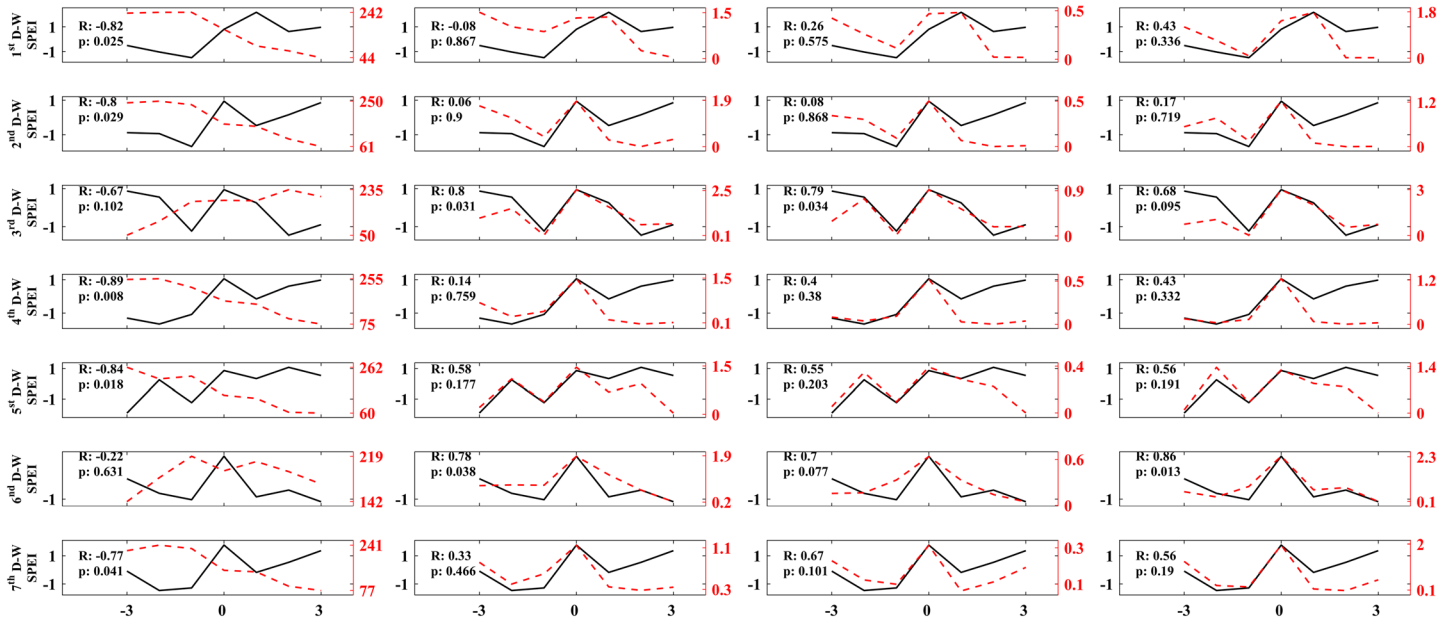

Figure 8. Interrelationships between dry-wet (D-W) alternation event and heavy rainfall with different intensities including R10–20, R20–25, and R25. Black lines represent the SPEI values. The red dashed lines represent the PET values in the first column, R10–20 values in the second column, which denotes the monthly number of days with daily precipitation ranging from 10 to 20 mm, R20–25 values in the third column, which denotes the monthly number of days with daily precipitation ranging from 20 to 25 mm, and R25 values in the fourth column, which denotes the monthly number of days with daily precipitation greater than 25 mm. *R* denotes the value of the Pearson correlation coefficient, and *p* denotes the *p* value derived by hypothesis testing with the significance level of 5%. The x ticks of −3 to 3 indicate 3 months before and 3 months after the occurrence of the D-W alternation event.

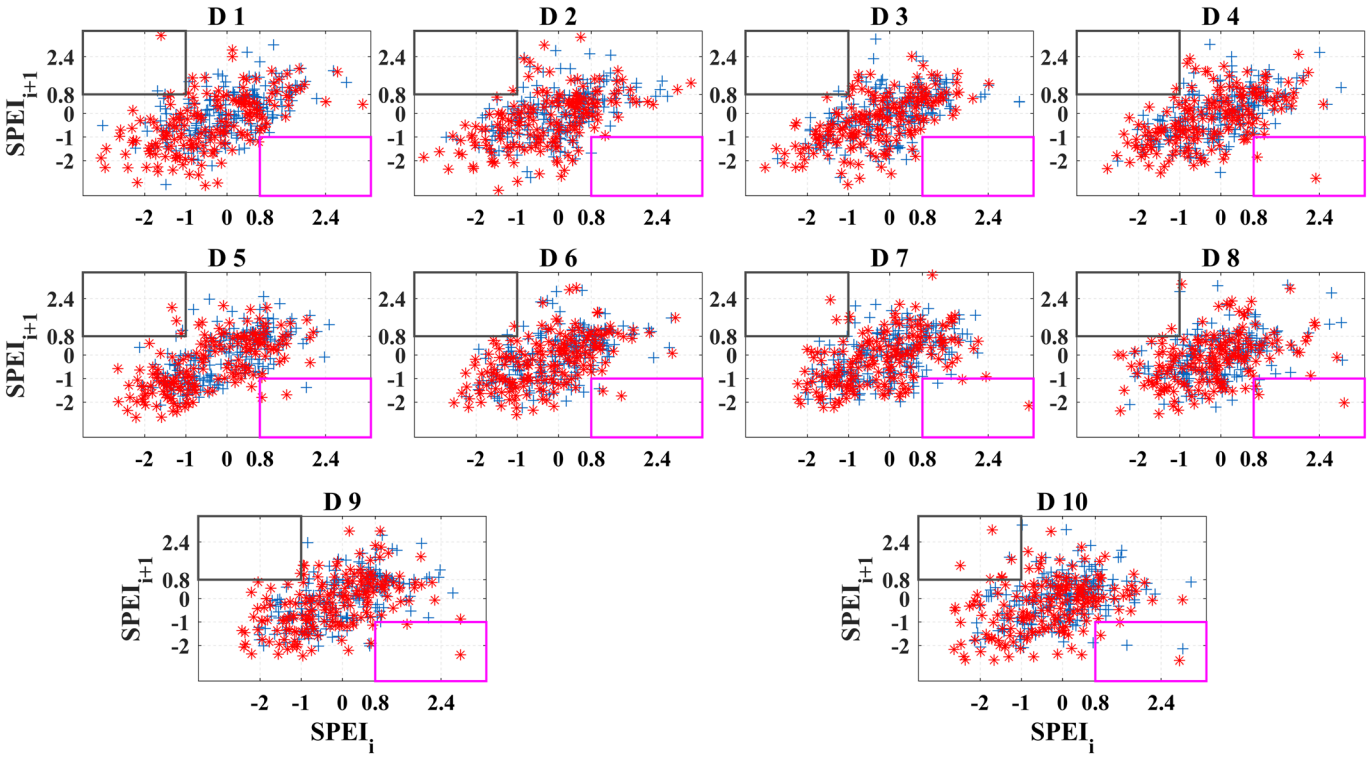

Figure 9. The number of historical (blue points) and future (red points) DWAA events derived by SPEI for 10 climate divisions of Texas. The points lying inside the pink rectangle represent the occurrence of the W-D alternation event, while the points lying inside the gray rectangle represent the occurrence of the D-W alternation event.

(Divisions 1 and 3) shows no occurrence and no change in the W-D alternation events as highlighted by pink rectangles.

Figure 10 depicts the comparison of historical and future DWAA events derived by SPEI for 10 climate divisions of Texas. It can be seen that the consecutive dry months leading up to the D-W alternation events (gray bars) persist at 1 or 2 months, except one consecutive dry spell that persists 4 months in Division 5 before the transition to wet spells in the historical period. In addition, more than half of future D-W alternation events are expected to have consecutive dry months more than 2 months, and the largest number of consecutive dry months leading up to the future D-W alternation is projected to be 6 months in Division 5. It is indicated that the number of consecutive dry months before a transition between wet and dry spells is projected to become larger than historical events, which can cause severe consequences. In addition, three DWAA events are projected to occur in neighboring divisions simultaneously. As shown in Figure 10, a D-W alternation event (gray bar) and a W-D alternation event (pink bar) are expected to occur simultaneously in Divisions 6 and 7, respectively. And a W-D alternation event (pink bar) is also projected to occur in Divisions 7–10 simultaneously. These results suggest that the DWAA events are expected not only to become more frequent but also to influence a larger spatial area of Texas in a changing climate, especially for the most populous region of South Texas where San Antonio and Austin are located.

Figure 11 shows the frequency distributions of historical and future monthly mean precipitation and PET for 10 climate divisions of Texas. The frequency distribution of precipitation indicates that heavy rainfall will become more frequent over Texas, especially in Divisions 2, 4, and 7–10 where there is a significant difference (at the significance level of 5% by F test) in the frequency of occurrence of historical and future heavy rainfall. Meanwhile, there is a considerable increase in the frequency of occurrence of high PET for all climate divisions of Texas, thereby increasing the likelihood for drought conditions. As a result, the increasing frequency of occurrence of heavy rainfall and high PET will lead to substantial variations in the DWAA characteristics.

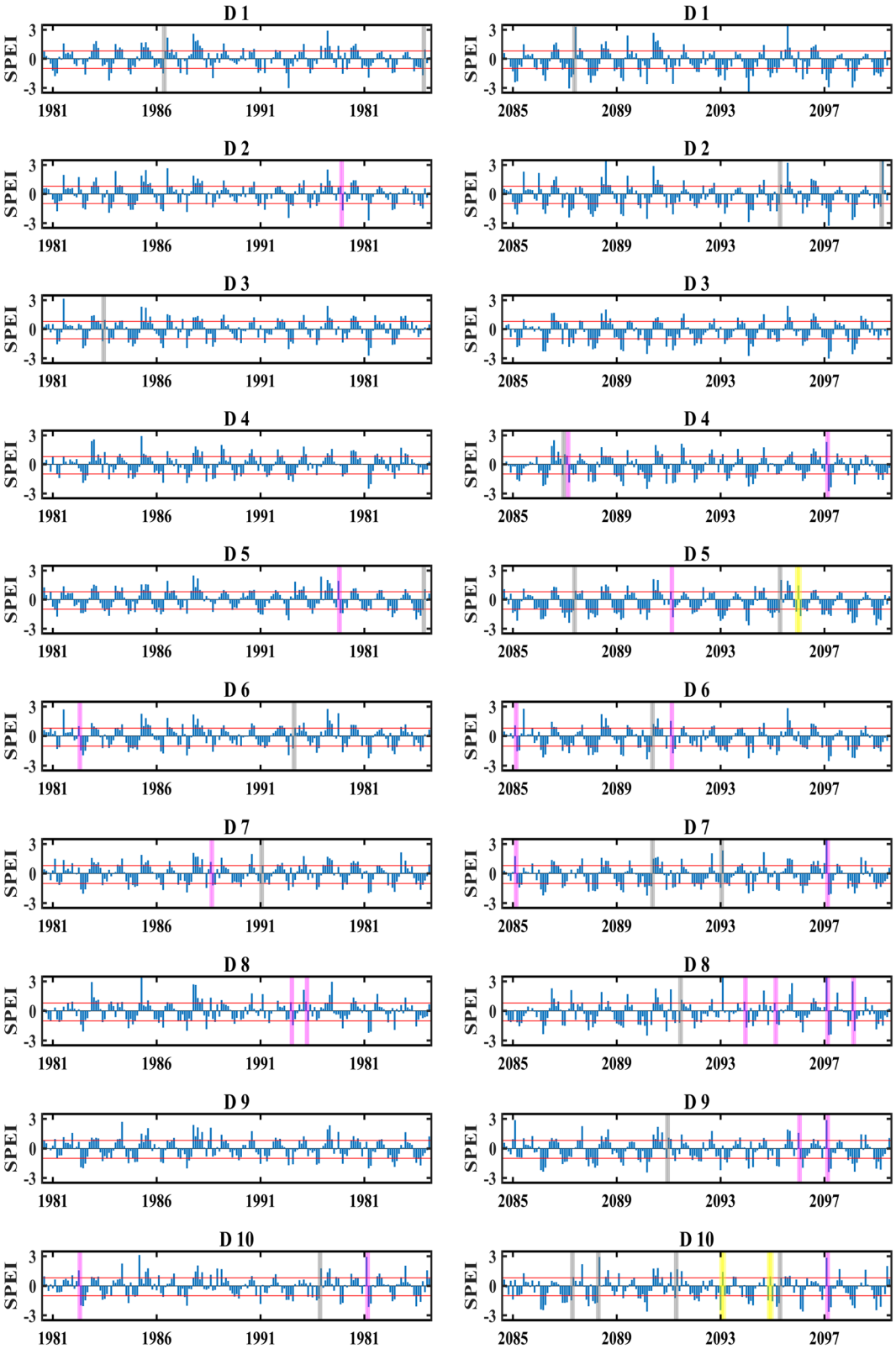

Figure 10. The number of DWAA events in the historical period (the first column) and the future period (the second column) for 10 climate divisions of Texas. The pink bar represents the occurrence of the W-D alternation event. The gray bar represents the occurrence of the D-W alternation event. The yellow bar represents the occurrence of the D-W-D alternation event.

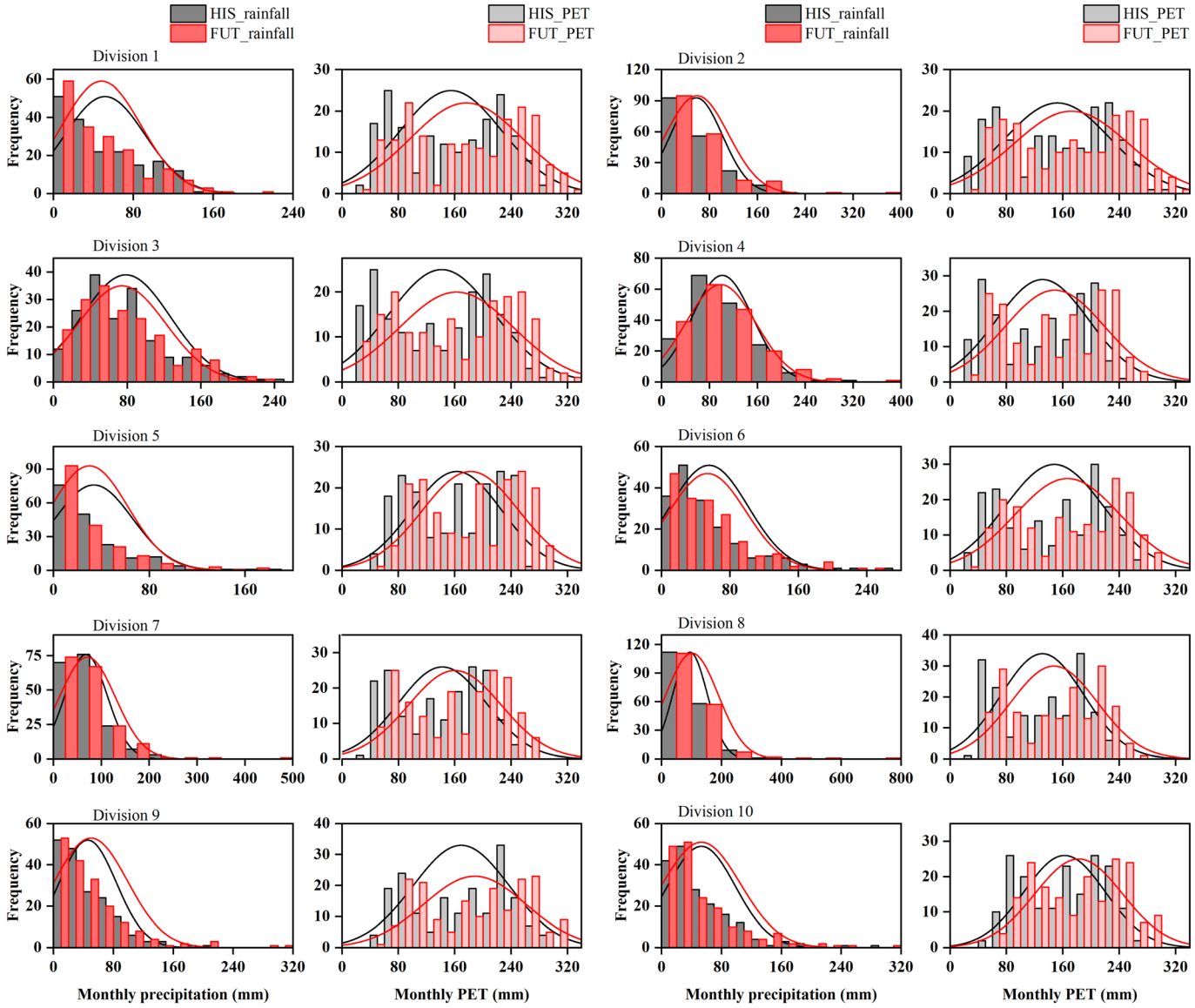

Figure 11. Changes in the frequency distributions of monthly mean rainfall and PET over 10 climate divisions of Texas for the historical period of 1981–1995 and the future period of 2085–2099. The gray bar represents the historical data, and the gray line represents the fitted frequency distribution for the historical period. The red bar represents the future data, and the red line represents the fitted frequency distribution for the future period.

Figure 12 presents the comparison of the number of days of historical (blue) and future (red) heavy rainfall with different intensities for 10 climate divisions of Texas. There is a significant decrease in the number of days of R10–20 and R20–25 categories for all climate divisions, whereas most climate divisions show an increase in the number of days of the R25 category. In addition, there is a significant positive shift for Divisions 2, 7, 8, and 9 at the significance level of 5%. It is indicated that the R25 has the most significant contribution to the W-D alternation. Thus, the increase in the number of days of R25 will lead to more frequent occurrence of the W-D alternation events for Central and South Texas (Divisions 7–9) that cover the areas of San Antonio, Austin, and Houston.

4. Discussions

Future changes of DWAA events as well as their interrelationships with heavy rainfall and PET have been projected through the convection-permitting climate simulations for 10 climate divisions over Texas. In

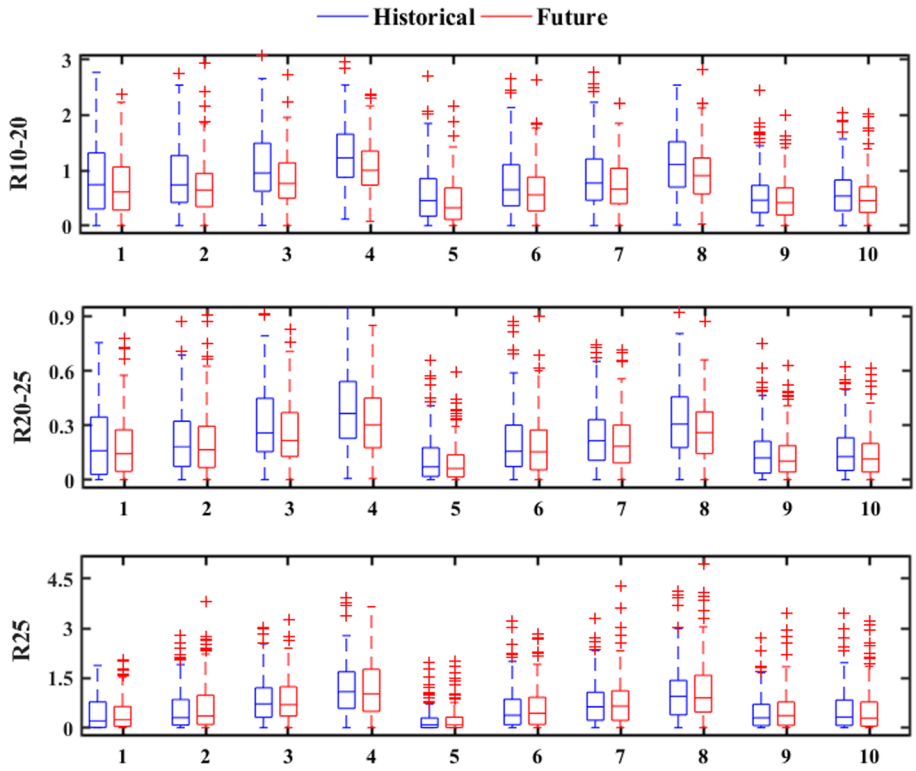

Figure 12. Changes in the monthly average number of historical (blue) and future (red) heavy rainfall with different intensities for 10 climate divisions of Texas.

general, the DWAA events are projected to occur more frequently over a larger spatial extent in a changing climate. In particular, the increasing frequency of occurrence of heavy rainfall with daily precipitation greater than 25 mm and high PET will lead to more frequent occurrence of the DWAA events.

DWAA has great potential risk for the loss of lives and economic damages (De Silva & Kawasaki, 2018; Lott & Ross, 2006). For instance, a W-D alternation event was detected in summer of 1987 over South Central (Division 7) that covered the areas of the two most populous cities including San Antonio and Austin. It was actually reported that a severe flood occurred in early summer of 1987 (1987 Guadalupe River Flood) and then turned into a meteorological drought in late summer of 1987 (Ross & Lott, 2003). In addition, a D-W alternation event was detected in fall of 1995 over West Texas (Division 5). It was reported that heavy rains fell in northwestern Texas where dry weather lasted since late 1995 (NOAA, 1996). These rains had a beneficial impact on the prolonged moisture deficits but engendered localized flash flooding as a result of concentrated precipitation during the week.

The WRF model suggests an increased likelihood that a severe super extreme event of dry-wet-dry (D-W-D) alternation (as highlighted by yellow bars in Figure 10) will appear by the end of this century, whereas there is no historical record on the occurrence of such an extreme event. The increasing extreme heavy rainfall at the expense of light rainfall is expected to increase the frequency of occurrence of the D-W-D alternation events which most likely occur in summer. In addition, the extended period of droughts can contribute to soil erosion (Allen et al., 2011), and nutrients at the surface of the soil can be washed away by heavy rainfall, thereby accelerating the *soil erosion process*. Furthermore, the excess water from heavy rainfall cannot be absorbed by the deteriorated soil due to the decreasing soil water holding capacity, thereby discharging into the river. Since the frequency of occurrence of R10–20 and R20–25 categories is expected to decrease (as shown in Figure 12) and there will be little change in the frequency of occurrence of the R25 category in Divisions 5 and 10, the D-W alternation caused by heavy rainfall can abruptly turn back into the dry condition due to the dry soil, resulting in the occurrence of the super extreme event of the D-W-D alternation in Divisions 5 and 10.

Dallas is the third most populous city in Texas, which is located in North Central (Division 3). There is only one historical record on the occurrence of the DWAA events for this region, and the convection-permitting climate simulation suggests that there is no such extreme event in the future. As shown in Figure 12, the average number of heavy rainfall events is projected to decrease for Division 3 in relative to the base period. This indicates that the frequency of occurrence of extreme precipitation is projected to decrease over North Central (Division 3), thereby leading to a relatively low risk of DWAA events. By contrast, the number of DWAA events is projected to increase over South Central (Division 7) where the most populous cities of San Antonio and Austin are located. In addition, the DWAA event is projected to occur more frequently over Upper Coast (Division 8) where the largest city of Houston is located. The projected future changes of DWAA provide meaningful insights into the evolution of climate-induced extreme events, which plays a crucial role in helping policymakers and stakeholders develop adaptation plans for reducing potential damages caused by climate-induced disasters.

5. Conclusions

In this study, the complex evolution of the emerging DWAA events was explored for 10 climate divisions over Texas. Future changes of DWAA were projected using the convection-permitting WRF model. In addition, the potential interrelationships of various types of DWAA and heavy rainfall with different intensities as well as PET were investigated thoroughly in order to advance the understanding of DWAA mechanisms and influencing factors.

Our findings reveal that DWAA is mainly attributed to the temporal and spatial variability of precipitation, especially for heavy rainfall with daily precipitation greater than 20 mm that contributes most to the W-D alternation events. Furthermore, a strong correlation between the D-W alternation event and PET is detected, whereas there is no significant correlation between the D-W alternation and extreme precipitation. The DWAA events are projected to occur more frequently over a larger area of Texas, especially for the most populous cities including San Antonio, Austin, and Houston. Due to the increasing number of drought and heavy rainfall events in a changing climate, a super extreme event of the D-W-D alternation is projected to appear by the end of this century, whereas there is no historical record on the occurrence of such an extreme event over Texas. It should be noted that the frequency of occurrence of extreme precipitation is projected to decrease over North Central (Division 3) where the third most populous city of Dallas is located, thereby leading to a relatively low risk of the DWAA events. The projected future changes of DWAA provide meaningful insights into the development of adaptation strategies for reducing potential risks of natural extreme events.

It should be noted that the high-resolution convection-permitting climate projection was conducted in this study under the business-as-usual scenario of RCP8.5; the projected future changes of the DWAA events would be different depending on future emission scenarios. For instance, the potential risk of DWAA would be reduced under the scenario with substantial greenhouse gas emission cuts (RCP4.5). In addition, the only two 15-year climate simulations are not long enough to robustly explore the dynamic evolution of natural disasters (DWAA). Future studies would thus be undertaken to conduct the longer-term convection-permitting climate simulation in order to improve the reliability and robustness of modeling results when computational resources become available.

Acknowledgments
This research was supported by the National Natural Science Foundation of China (Grant 51809223) and the Hong Kong Polytechnic University Start-up Grant (Grant 1-ZE8S). The precipitation, PET, and heavy rainfall variables derived from the WRF model and the PRISM observations can be accessed online (https://data.mendeley.com/datasets/fwpspnxtw9/1). We would like to express our sincere gratitude to the Editor and three anonymous reviewers for their constructive comments and suggestions.

References

Ahmed, K. F., Wang, G., Silander, J., Wilson, A. M., Allen, J. M., Horton, R., & Anyah, R. (2013). Statistical downscaling and bias correction of climate model outputs for climate change impact assessment in the U.S. northeast. *Global and Planetary Change*, *100*, 320–332. https://doi.org/10.1016/j.gloplacha.2012.11.003

Alexander, L. V., Zhang, X., Peterson, T. C., Caesar, J., Gleason, B., Klein Tank, A. M. G., et al. (2006). Global observed changes in daily climate extremes of temperature and precipitation. *Journal of Geophysical Research*, *111*, D05109. https://doi.org/10.1029/2005JD006290

Allen, P. M., Harmel, R. D., Dunbar, J. A., & Arnold, J. G. (2011). Upland contribution of sediment and runoff during extreme drought: A study of the 1947–1956 drought in the Blackland Prairie, Texas. *Journal of Hydrology*, *407*(1), 1–11.

Allen, R. G., Walter, I. A., Elliot, R. L., Howell, T. A., Itenfisu, D., Jensen, M. E., & Snyder, R. (2005). The ASCE standardized reference evapotranspiration equation. *ASCE and American Society of Civil Engineers*.

Azizzadeh, M. R., & Javan, K. (2018). Temporal and spatial distribution of extreme precipitation indices over the lake Urmia Basin, Iran. *Environmental Resources Research*, *6*(1), 25–40.

Christian, J., Christian, K., & Basara, J. B. (2015). Drought and pluvial dipole events within the Great Plains of the United States. *Journal of Applied Meteorology and Climatology*, *54*, 1886–1898.

Clark, J. S., Campbell, J. H., Grizzle, H., Acosta-Martìnez, V., & Zak, J. C. (2009). Soil microbial community response to drought and precipitation variability in the Chihuahuan Desert. *Microbial Ecology*, *57*(2), 248–260. https://doi.org/10.1007/s00248-008-9475-7

Cordova, C. E. (2000). Geomorphological evidence of intense prehistoric soil erosion in the highlands of central Jordan. *Physical Geography*, *21*(6), 538–567.

Daly, C., Halbleib, M., Smith, J. I., Gibson, W. P., Doggett, M. K., Taylor, G. H., et al. (2008). Physiographically sensitive mapping of climatological temperature and precipitation across the conterminous United States. *International Journal of Climatology: A Journal of the Royal Meteorological Society*, *28*(15), 2031–2064. https://doi.org/10.1002/joc.1688

De Silva, M. M. G. T., & Kawasaki, A. (2018). Socioeconomic vulnerability to disaster risk: A case study of flood and drought impact in a rural Sri Lankan community. *Ecological Economics*, *152*, 131–140.

Dong, X., Xi, B., Kennedy, A., Feng, Z., Entin, J. K., Houser, P. R., et al. (2011). Investigation of the 2006 drought and 2007 flood extremes at the Southern Great Plains through an integrative analysis of observations. *Journal of Geophysical Research*, *116*, D03204. https://doi.org/10.1029/2010JD014776

Du, J., Fang, J., Xu, W., & Shi, P. (2013). Analysis of dry/wet conditions using the standardized precipitation index and its potential usefulness for drought/flood monitoring in Hunan Province, China. *Stochastic Environmental Research and Risk Assessment*, *27*(2), 377–387.

Frich, P., Alexander, L., Della-Marta, P., Gleason, B., Haylock, M., Amg Klein, T., & Tc, P. (2002). Observed coherent changes in climatic extremes during 2nd half of the 20th century. *Climate Research*, *19*(3), 193–212.

Guo, X., Huang, J., Luo, Y., Zhao, Z., & Xu, Y. (2016). Projection of precipitation extremes for eight global warming targets by 17 CMIP5 models. *Natural Hazards*, *84*(3), 2299–2319.

Handwerger, A. L., Huang, M. H., Fielding, E. J., Booth, A. M., & Bürgmann, R. (2019). A shift from drought to extreme rainfall drives a stable landslide to catastrophic failure. *Scientific Reports*, *9*(1), 1569. https://doi.org/10.1038/s41598-018-38300-0

Hong, S. Y., & Pan, H. L. (1996). Nonlocal boundary layer vertical diffusion in a medium-range forecast model. *Monthly Weather Review*, *124*(10), 2322–2339.

Iacono, M. J., Delamere, J. S., Mlawer, E. J., Shephard, M. W., Clough, S. A., & Collins, W. D. (2008). Radiative forcing by long-lived greenhouse gases: Calculations with the AER radiative transfer models. *Journal of Geophysical Research*, *113*, D13103. https://doi.org/10.1029/2008JD009944

Ji, Z., Li, N., & Wu, X. (2018). Threshold determination and hazard evaluation of the disaster about drought/flood sudden alternation in Huaihe River basin, China. *Theoretical and Applied Climatology*, *133*(3–4), 1279–1289.

Jiménez, P. A., Dudhia, J., González-Rouco, J. F., Navarro, J., Montávez, J. P., & García-Bustamante, E. (2012). A revised scheme for the WRF surface layer formulation. *Monthly Weather Review*, *140*(3), 898–918.

Katsanos, D., Retalis, A., Tymvios, F., & Michaelides, S. (2018). Study of extreme wet and dry periods in Cyprus using climatic indices. *Atmospheric Research*, *208*, 88–93.

Liu, C., Ikeda, K., Rasmussen, R., Barlage, M., Newman, A. J., Prein, A. F., et al. (2017). Continental-scale convection-permitting modeling of the current and future climate of North America. *Climate Dynamics*, *49*(1–2), 71–95. https://doi.org/10.1007/s00382-016-3327-9

Liu, C., Ikeda, K., Thompson, G., Rasmussen, R., & Dudhia, J. (2011). High-resolution simulations of wintertime precipitation in the Colorado Headwaters region: Sensitivity to physics parameterizations. *Monthly Weather Review*, *139*, 3533–3553.

Lott, N., & Ross, T. (2006). 1.2 tracking and evaluating US billion dollar weather disasters, 1980-2005, Asheville, NC: NOAA National Climatic Data Center.

Malik, N., Bookhagen, B., & Mucha, P. J. (2016). Spatiotemporal patterns and trends of Indian monsoonal rainfall extremes. *Geophysical Research Letters*, *43*(4), 1710–1717. https://doi.org/10.1002/2016GL067841

McKee, T. B., Doesken, N. J., & Kleist, J. (1993). The relationship of drought frequency and duration to time scales, *in Proceedings of the 8th Conference on Applied Climatology*, *American Meteorological Society*, Boston, Mass.

Mishra, A., & Liu, S. C. (2014). Changes in precipitation pattern and risk of drought over India in the context of global warming. *Journal of Geophysical Research: Atmospheres*, *119*, 7833–7841. https://doi.org/10.1002/2014JD021471

Mo, K. C. (2011). Drought onset and recovery over the United States. *Journal of Geophysical Research*, *116*, D20106. https://doi.org/10.1029/2011JD016168

Nalbantis, I., & Tsakiris, G. (2009). Assessment of hydrological drought revisited. *Water Resources Management*, *23*(5), 881–897.

Niu, G. Y., Yang, Z. L., Mitchell, K. E., Chen, F., Ek, M. B., Barlage, M., et al. (2011). The community Noah land surface model with multiparameterization options (Noah-MP): 1. Model description and evaluation with local-scale measurements. *Journal of Geophysical Research*, *116*, D12109. https://doi.org/10.1029/2010JD015139

NOAA (1996). Global climate highlights major events and anomalies as of June 29, 1996. The climate bulletin. No.96/7. p.7.

Prein, A. F., Rasmussen, R. M., Ikeda, K., Liu, C., Clark, M. P., & Holland, G. J. (2016). The future intensification of hourly precipitation extremes. *Nature Climate Change*, *7*, 48.

Rasmussen, K. L., Prein, A. F., Rasmussen, R. M., Ikeda, K., & Liu, C. (2017). Changes in the convective population and thermodynamic environments in convection-permitting regional climate simulations over the United States. *Climate Dynamics*. https://doi.org/10.1007/s00382-017-4000-7

Ross, T., & Lott, N. (2003). A climatology of 1980-2003 extreme weather and climate events, National Climatic Data Center Technical Report, 01.

Schmidt, M., Lucke, B., Bäumler, R., al-Saad, Z., al-Qudah, B., & Hutcheon, A. (2006). The Decapolis region (Northern Jordan) as historical example of desertification? Evidence from soil development and distribution, *Quaternary International*, *151*(1), 74–86.

Shan, L., Zhang, L., Song, J., Zhang, Y., She, D., & Xia, J. (2018). Characteristics of dry-wet abrupt alternation events in the middle and lower reaches of the Yangtze River Basin and the relationship with ENSO. *Journal of Geographical Sciences*, *28*(8), 1039–1058.

Singh, D., Tsiang, M., Rajaratnam, B., & Diffenbaugh, N. S. (2014). Observed changes in extreme wet and dry spells during the South Asian summer monsoon season. *Nature Climate Change*, *4*, 456.

Skamarock, W. C., Klemp, J. B., Dudhia, J., Gill, D. O., Barker, D. M., Duda, M. G., et al. (2008). A description of the advanced research WRF version. *3*.

Thompson, G., Field, P. R., Rasmussen, R. M., & Hall, W. D. (2008). Explicit forecasts of winter precipitation using an improved bulk microphysics scheme. Part II: Implementation of a new snow parameterization. *Monthly Weather Review*, *136*(12), 5095–5115.

Vicente-Serrano, S. M., Beguería, S., & López-Moreno, J. I. (2010). A multiscalar drought index sensitive to global warming: The standardized precipitation evapotranspiration index. *Journal of Climate*, *23*(7), 1696–1718.

Wang, G., Wang, D., Trenberth, K. E., Erfanian, A., Yu, M., Bosilovich, M. G., & Parr, D. T. (2017). The peak structure and future changes of the relationships between extreme precipitation and temperature. *Nature Climate Change*, *7*, 268.

Wang, S., Ancell, B., Huang, G., & Baetz, B. (2018). Improving robustness of hydrologic ensemble predictions through probabilistic pre-and post-processing in sequential data assimilation. *Water Resources Research*, *54*, 2129–2151. https://doi.org/10.1002/2018WR022546

Wang, S., & Wang, Y. (2019). Improving probabilistic hydroclimatic projections through high-resolution convection-permitting climate modeling and Markov chain Monte Carlo simulations. *Climate Dynamics*, *53*(3), 1613–1636.

Wang, S., & Zhu, J. (2020). Amplified or exaggerated changes in perceived temperature extremes under global warming. *Climate Dynamics*, *54*, 117–127.

Wang, S.-Y. S., Huang, W.-R., Hsu, H.-H., & Gillies, R. R. (2015). Role of the strengthened El Niño teleconnection in the May 2015 floods over the southern Great Plains. *Geophysical Research Letters*, (42), 8140–8146. https://doi.org/10.1002/2015GL065211

Wu, Z., Li, J., He, J., & Jiang, Z. (2006). Occurrence of droughts and floods during the normal summer monsoons in the mid- and lower reaches of the Yangtze River. *Geophysical Research Letters*, *33*, L05813.

Yang, Z. L., Niu, G. Y., Mitchell, K. E., Chen, F., Ek, M. B., Barlage, M., et al. (2011). The community Noah land surface model with multiparameterization options (Noah-MP): 2. Evaluation over global river basins. *Journal of Geophysical Research*, *116*, D12110. https://doi.org/10.1029/2010JD015140

Yoon, J.-H., Wang, S. Y. S., Lo, M.-H., & Wu, W.-Y. (2018). Concurrent increases in wet and dry extremes projected in Texas and combined effects on groundwater. *Environmental Research Letters*, *13*, 054002.

Zhang, B., Wang, S., & Wang, Y. (2019). Copula-based convection-permitting projections of future changes in multivariate drought characteristics. *Journal of Geophysical Research: Atmospheres*, *124*, 7460–7483. https://doi.org/10.1029/2019JD030686

Zhang, Y., Jiang, F., Wei, W., Liu, M., Wang, W., Bai, L., et al. (2012). Changes in annual maximum number of consecutive dry and wet days during 1961–2008 in Xinjiang, China. *Natural Hazards and Earth System Sciences*, *12*(5), 1353–1365.

Zhu, J., Wang, S., & Huang, G. (2019). Assessing climate change impacts on human-perceived temperature extremes and underlying uncertainties. *Journal of Geophysical Research: Atmospheres*, *124*, 3800–3821. https://doi.org/10.1029/2018JD029444